Author's response

Manuscript: "Enhanced summertime ozone and SOA from biogenic volatile organic compound (BVOC) emissions due to vegetation biomass variability during 1981–2018 in China" (acp-2021-675)

Responses to reviewers' comments are listed below, respectively. Revised portions are marked in red.

Response to Referee #1

1. Model evaluation should be added. The authors should show evidences to make the results convincing, especially the BVOC emissions.

Response: Thank you so much for your suggestion. In revised manuscript, we add the model evaluations.

(1) Validation of BVOC emission simulations by MEGAN.

Firstly, we compared the estimation with canopy-level emission flux measurements in China (Bai et al., 2015, 2016, 2017). The gridded BVOC emission estimated by MEGAN were extracted where locating the flux measurement sites. The comparison of model simulation and observation is shown in Fig. S1. The estimated BVOC emissions are higher with an average mean bias of 1.11 mg m^{-2} h^{-1}, mainly because of the differences in time between the simulation and measurements. But they are correlated by r=0.84, exhibiting good agreement in spatial variations.

Secondly, formaldehyde (HCHO) concentrations observed by satellite were used to evaluate the spatial variability of estimated isoprene emissions. Isoprene is the dominant compound among BVOC species that accounts for almost half of total BVOC emissions in China. Since HCHO is an important proxy of isoprene in forest regions with no significant anthropogenic impact, satellite HCHO observations can be used to validate the spatial variability of biogenic isoprene emissions. We compared simulated isoprene emission with

satellite-derived HCHO column concentration using the Ozone Monitoring Instrument (OMI) HCHO vertical column product. The monthly averaged OMI HCHO vertical column in June 2018 correlates with the model estimated results at a 99% confidence level.

Line 171–185 of revised manuscript, "The emission simulations were validated by using the measurements of BVOC emission flux and formaldehyde (HCHO) concentration. The flux measurements of BVOCs conducted in China were collected (Bai et al., 2015, 2016, 2017). The gridded BVOC emission estimated by MEGAN were extracted where the flux measurement sites were located to do the comparison (Fig. S1). The modeled fluxes of BVOCs in this study capture the spatial variability of observations better with a correlation coefficient of 0.84. But the estimation is higher than measurement with an average mean bias of 1.11 mg m^{-2} h^{-1}, mainly because of the differences in time between them. Isoprene is the main compound in BVOC species, accounting for nearly half of total BVOC emissions in China. It undergoes chemical and photochemical reactions in the atmosphere, and the oxidation product is mainly HCHO (Bai and Hao, 2018; Orlando et al., 2000). In forest areas and in summer, biogenic isoprene is the dominant source of HCHO, so satellite HCHO column concentration is widely used to constrain isoprene emissions (Opacka et al., 2021; Palmer et al., 2003; Stavrakou et al., 2018; Wang et al., 2021; Zhang et al., 2021). In this study, we used the HCHO vertical column detected by Ozone Monitoring Instrument (OMI) to validate the spatial variability of isoprene estimates. The monthly OMI HCHO data from the EU FP7 project QA4ECV product (Quality Assurance for Essential Climate Variables; http://www.qa4ecv.eu) was used in this study. The result of the statistical analysis with a confidence interval of 99% indicates that the monthly averaged OMI HCHO vertical column in June 2018 is significantly correlated to the model-estimated isoprene emissions." is added.

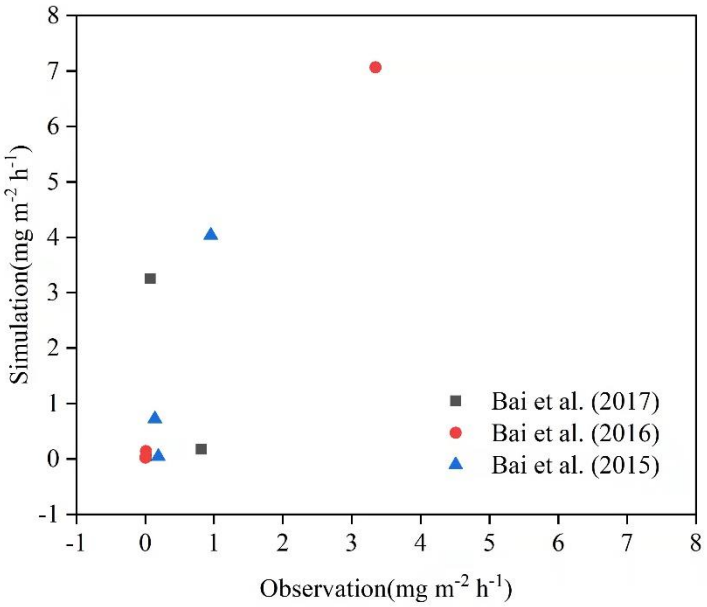

Fig. S1. Comparison of MEGAN model simulations with flux measurements in China.

(2) Validation of meteorological data simulated by WRF.

Temperature and radiation play key roles in BVOC emissions. The observations of temperature at 2411 sites in 2008 and 684 sites in 2018 in China were used to compare with WRF-simulated 2-m temperature (T2). The simulated radiation was not evaluated because of a lack of available site observations. In the revised manuscript, we add the validation for WRF simulation. Meanwhile, to make the description more clear, the statement of MEGAN in Section 2.1 is reorganized.

Line 87–96, "Meteorology, gridded fraction of plant functional types (PFTs), PFT-specific emission factors, and leaf area index (LAI) are inputs to drive MEGAN. MODIS LAI data was used. The hourly meteorological fields including temperature, downward shortwave radiation, wind speed, water vapor mixing ratio, pressure, and precipitation were simulated by the WRF model in this study. The WRF-simulated meteorological fields were verified to be considered reasonable for driving MEGAN (Li et al., 2013, 2021)." is revised to "MEGAN2.1 requires hourly weather variables to drive the calculation of hourly BVOC emissions. The hourly meteorological fields including temperature, downward shortwave radiation, wind speed, water vapor mixing ratio, pressure, and precipitation were simulated by the WRF model in this study. Temperature and radiation play key roles in BVOC emissions. We used the observed daily

average temperature at 2411 sites in 2008 and 684 sites in 2018 in China to evaluate the reliability of the 2-m temperature (T2) simulated by WRF in this study. The observations were from the National Meteorological Data Center in China (http://data.cma.cn/). The simulated radiation was not evaluated because of a lack of available site observations. For 2008, the average mean bias (MB), mean absolute error (MAE), and root-mean-square error (RMSE) are 0.36, 2.47, and 3.30 K over China. For 2018, these statistics are 1.24, 2.46 and 3.30 K, respectively. The correlation coefficients between simulations and observations are 0.82 and 0.86 for the year 2008 and 2018, respectively. In general, the WRF simulation is considered reasonable for driving MEGAN.". Line 87, "Meteorological and vegetation data are inputs to drive MEGAN." is added. Line 96–98, "The vegetation data includes gridded fraction of plant functional types (PFTs), leaf area index (LAI), and PFT-specific emission factors." is added. Line 103, "For LAI, the MODIS LAI data was used." is added.

(3) Validation of O_3 and SOA simulations by WRF-Chem.

In this study, we aim to explore the impact of interannual BVOC emission variations on O_3 and SOA caused by vegetation biomass variability. The historical O_3 and SOA concentrations were simulated by fixing the anthropogenic emissions and meteorological data in 2008. So we did not conduct validation for WRF-Chem simulation. However, WRF-Chem model has been widely used in global and regional pollution studies and verified to have a good performance on the simulation of secondary pollutants(Gupta and Mohan, 2015; Hoshyaripour et al., 2016; Li et al., 2018; Situ et al., 2013; Wu et al., 2018).

Line 129–131 of revised manuscript, "A large number of global and regional air pollution studies widely apply it to simulate secondary pollutants, and the verification results show that it can well reproduce the observed pollutant concentrations (Gupta and Mohan, 2015; Hoshyaripour et al., 2016; Li et al., 2018; Situ et al., 2013; Wu et al., 2018)." is added.

In addition, the uncertainty by fixing the anthropogenic emissions and meteorological data in 2008 is also added in the revised manuscript. Line 402–410, "In this study, we aim to explore the impact of interannual BVOC emission variations on O_3 and SOA caused by vegetation biomass variability. The historical O_3 and SOA concentrations were simulated by fixing the anthropogenic emissions and meteorological data in 2008. The influences of annual meteorology on BVOC emissions and formation of secondary air pollutants were not

considered. Although vegetation change is the main driver of interannual variations of BVOC emissions, it still brings uncertainty to the simulation in this study. Future work can update the anthropogenic emission inventory and use dynamic meteorological data to explore multivariate effects and provide more accurate data for evaluating the roles of biogenic emissions in air quality. At the same time, the impact of meteorological changes on the long-term changes of BVOC emissions and formation of secondary air pollutants should also be considered to provide a scientific basis for the precise prevention and control of air pollution in response to climate change." is added.

References:

Bai, J.H. and Hao, N.: The relationships between biogenic volatile organic compound (BVOC) emissions and atmospheric formaldehyde in a subtropical Pinus plantation in China, Ecology and Environmental Sciences, 27(6): 991–999, https://doi.org/10.16258/j.cnki.1674-5906.2018.06.001, 2018.

Bai, J., Guenther, A., Turnipseed, A., and Duhl, T.: Seasonal and interannual variations in whole-ecosystem isoprene and monoterpene emissions from a temperate mixed forest in Northern China, Atmos. Pollut. Res., 6, 696–707, https://doi.org/10.5094/APR.2015.078, 2015.

Bai, J., Guenther, A., Turnipseed, A., Duhl, T., Y u, S., and Wang, B.: Seasonal variations in whole-ecosystem BVOC emissions from a subtropical bamboo plantation in China, Atmos. Environ., 124, 12–21, https://doi.org/10.1016/j.atmosenv.2015.11.008, 2016.

Bai, J., Guenther, A., Turnipseed, A., Duhl, T., and Greenberg, J.: Seasonal and interannual variations in whole-ecosystem BVOC emissions from a subtropical plantation in China, Atmos. Environ., 161, 176–190, https://doi.org/ 10.1016/j.atmosenv.2017.05.002, 2017.

Gupta, M. and Mohan, M.: Validation of WRF/Chem model and sensitivity of chemical mechanisms to ozone simulation over megacity Delhi, Atmos. Environ., 122, 220–229, 2015.

Hoshyaripour, G., Brasseur, G., Andrade, M.F., Gavidia-Calder, M., Bouarar, I., Ynoue, R.Y.: Prediction of ground-level ozone concentration in Sao Paulo, Brazil: deterministic versus

statistic models, Atmos. Environ., 145, 365–375, https://doi.org/10.1016/j.atmosenv.2016.09.061, 2016.

Li, N., He, Q., Greenberg, J., Guenther, A., Li, J., Cao, J., Wang, J., Liao, H., Wang, Q., and Zhang, Q.: Impacts of biogenic and anthropogenic emissions on summertime ozone formation in the Guanzhong Basin, China, Atmos. Chem. Phys., 18, 7489–7507, https://doi.org/10.5194/acp-18-7489-2018, 2018.

Opacka, B., Müller, J.-F., Stavrakou, T., Bauwens, M., Sindelarova, K., Markova, J., and Guenther, A. B.: Global and regional impacts of land cover changes on isoprene emissions derived from spaceborne data and the MEGAN model, Atmos. Chem. Phys., 21, 8413–8436, https://doi.org/10.5194/acp-21-8413-2021, 2021.

Orlando, J. J., Nozière, B., Tyndall, G. S., Orzechowska, G. E., Grazyna, E., Paulson, S. E., and Rudich Y.: Product studies of the OH- and ozone-initiated oxidation of some monoterpenes, J. Geophys. Res., 105, 11561–11572, https://doi.org/10.1029/2000JD900005, 2000.

Palmer, P . I., Jacob, D. J., Fiore, A. M., Martin, R. V ., Chance, K., and Kurosu, T. P .: Mapping isoprene emissions over North America using formaldehyde column observations from space, J. Geophys. Res.-Atmos., 108, 4180, https://doi.org/10.1029/2002JD002153, 2003.

Situ, S., Guenther, A., Wang, X., Jiang, X., Turnipseed, A., Wu, Z., Bai, J., and Wang, X.: Impacts of seasonal and regional variability in biogenic VOC emissions on surface ozone in the Pearl River Delta region, China, Atmos. Chem. Phys., 13, 11803–11817, https://doi.org/10.5194/acp-13-11803-2013, 2013.

Stavrakou, T., Müller, J.-F., Bauwens, M., De Smedt, I., Van Roozendael, M., and Guenther, A.: Impact of Short-Term Climate Variability on Volatile Organic Compounds Emissions Assessed Using OMI Satellite Formaldehyde Observations, Geophys. Res. Lett., 45, 8681–8689, 2018.

Wang, H., Wu, Q. Z., Guenther, A. B., Yang, X. C., Wang, L. N., Xiao, T., Li, J., Feng, J. M., Xu, Q., and Cheng, H.: A long-term estimation of biogenic volatile organic compound (BVOC) emission in China from 2001–2016: the roles of land cover change and climate variability, Atmos. Chem. Phys., 21, 4825–4848, https://doi.org/10.5194/acp-21-4825-

2021, 2021.

Wu, J., Bei, N., Li, X., Cao, J., Feng, T., Wang, Y., Tie, X., and Li, G.: Widespread air pollutants of the North China Plain during the Asian summer monsoon season: a case study, Atmos. Chem. Phys., 18, 8491–8504, https://doi.org/10.5194/acp-18-8491-2018, 2018.

Zhang, M., Zhao, C., Yang, Y., Du, Q., Shen, Y., Lin, S., Gu, D., Su, W., and Liu, C.: Modeling sensitivities of BVOCs to different versions of MEGAN emission schemes in WRF-Chem (v3.6) and its impacts over eastern China, Geosci. Model Dev., 14, 6155–6175, https://doi.org/10.5194/gmd-14-6155-2021, 2021.

2. The manuscript focused on the change of background O_3 and SOA in China due to the change of vegetation The MS should show the change of biomass as well as how the biomass changes affecting BVOC emissions.

Response: Thank you very much for your valuable suggestion. In revised manuscript, we add a new Section of "**3.1 BVOC emission**", in which "**3.1.2 Influence of leaf biomass variability**" describes the interannual variation of leaf biomass and its influence on BVOC emissions. The added Section 3.1.2 is as follows.

"**3.1.2 Influence of leaf biomass variability**

The leaf biomasses increased from 378.35 × 10^{12} g in 1981 to 1107.16 × 10^{12} g in 2018 at an average rate of 17.97 × 10^{12} g yr^{-1}. Among them, the forest and crop leaf biomass increased from 237.10 × 10^{12} to 518.38 × 10^{12} g and from 141.25 × 10^{12} to 588.79 × 10^{12} g, respectively, totally increasing by 192.63%. The spatial distribution of interannual variations in leaf biomass is presented in Fig. S2. The increase of leaf biomass is most significant in Great Khingan, Changbai Mountains, North China Plain, south and southwest China. This is mainly due to the increased stock of broadleaf and coniferous forests as a result of afforestation. Northern Qinghai-Tibet area and Northwest China have a relatively high grass cover rate but insignificant increase in leaf biomass of vegetation. It is because that the grass biomasses were the same over the historical simulations due to lacking of data.

Due to the increased volume and production of vegetation, the total BVOC emissions

increased by 58.66% at average rates of 96.64 Gg yr^{-1}, of which isoprene, monoterpene, sesquiterpene increased by 108.57%, 38.17%, and 33.35% at average rates of 11.10, 0.99, and 0.17 Gg yr^{-1}, respectively. Isoprene emissions increased more rapidly over the past 40 years, which is primarily due to the greater increase in the biomass of broadleaf trees, which have the highest isoprene emission rates. Monoterpene and sesquiterpene increased at a lower rate because the increase of leaf biomass of conifers is relatively small. Fig. 2 shows the spatial distribution of interannual variations in BVOC emissions caused by the changing leaf biomass. Since the needleleaf and broadleaf trees tend to have a higher emission potential than grass or crop (Guenther et al., 2012), their wide distribution and the substantial increase in biomass result in the largest interannual variability of BVOC emissions in the Great Khingan, Changbai Mountains, North China Plain, Central and Southern China, and Hainan Province. However, the emission of BVOCs in the northwest and southern coastal areas has decreased.

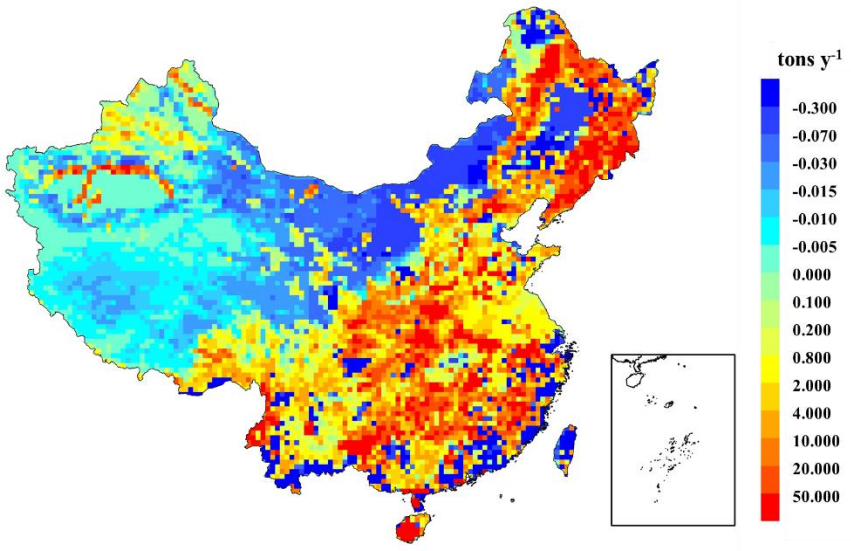

Fig. 2. Spatial distribution of interannual variations in BVOC emissions caused by leaf biomass changes."

Line 310–314, "The change of vegetation leaf biomass will cause the interannual variation of BVOCs emissions and then O_3 and SOA generation. During 1981–2018, the forest and crop leaf biomass increased from 237.10 × 10^{12} g to 518.38 × 10^{12} g and from 141.25 × 10^{12} g to 588.79 × 10^{12} g, respectively, totally increasing by 192.63%. In this study, the annual emission factors extrapolated from emission rates and annual leaf biomass were used to simulate the impact of interannual variation in BVOC emissions on O_3 and SOA, as described in Scenario

“HISTORY”." is deleted.

Figure S2 is added to the Supplementary File.

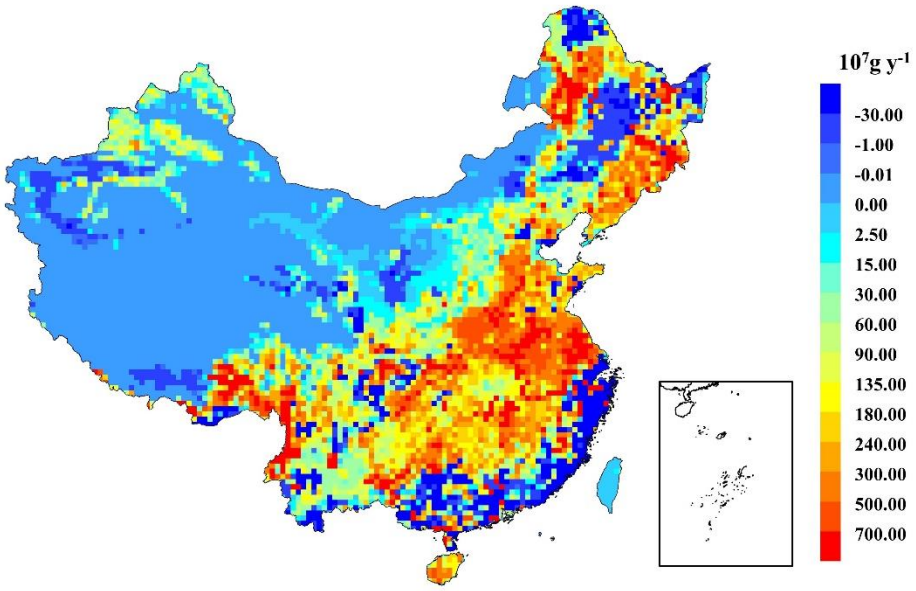

Fig. S2. Spatial distribution of interannual variations in leaf biomass.

References:

Guenther, A. B., Jiang, X., Heald, C. L., Sakulyanontvittaya, T., Duhl, T., Emmons, L. K., and Wang, X.: The model of emissions of gases and aerosols from nature version 2.1 (MEGAN2.1): an extended and updated framework for modeling biogenic emissions, Geosci. Model Dev., 5, 1471–1492, https://doi.org/10.5194/gmd-5-1471-2012, 2012.

3. The history simulation setting is not reasonable by fixing the meteorology in 2008 (as listed in Table 1). Why 2008 was chosen in this study? The BVOC emissions are very sensitive to meteorology change, and the meteorology is an important factor influencing the emission and air quality. Fixing the meteorology may induce the unreasonable results which should be discussed in the MS. Many factors influencing the BVOC emissions and their atmospheric chemistry in the past 4 decades. A method should be set to clarify the multivariate effects.

Response: Thank you so much for your valuable suggestion. As your comment, meteorology is an important factor that can influence both BVOC emissions and air quality. In our study, we aim to explore the impacts of interannual BVOC emission variations on O_3 and

SOA formation caused by vegetation biomass variability during 1981–2018. In order to achieve this goal, we designed a scenario experiment by fixing meteorological data in one year and using the annual leaf biomass to drive BVOC estimates. The influences of annual meteorology on BVOC emissions and formation of secondary air pollutants were not considered. It is reported that vegetation change is the main driver of interannual variations of BVOC emissions (Li et al., 2020; Wang et al., 2021). The large-scale afforestation activities in recent years lead to the rapid increase of vegetation leaf biomass and therein BVOC emissions. In addition, China's annual average temperature has a heating rate of 0.26 K per 10 years from 1951 to 2020 (Climate Change Center of China Meteorological Administration, 2021). Taking into account the long-term warming trend, we chose meteorological data of a mid-year 2008 over 1981–2018 as the constant input for historical simulation. Despite this, uncertainty is inevitable.

In the revised manuscript, we add the explanation for fixing meteorology in 2008 and discuss the uncertainty. Line 159–162, "For the meteorology, the fixing set of a mid-year 2008 over 1981–2018 were used for all the HISTORY simulations. To explore the impacts of interannual BVOC emission variations caused by vegetation biomass variability, influences of annual meteorology on BVOC emissions and formation of secondary air pollutants were not considered." is added.

Line 402–410, "In this study, we aim to explore the impact of interannual BVOC emission variations on O_3 and SOA caused by vegetation biomass variability. The historical O_3 and SOA concentrations were simulated by fixing the anthropogenic emissions and meteorological data in 2008. The influences of annual meteorology on BVOC emissions and formation of secondary air pollutants were not considered. Although vegetation change is the main driver of interannual variations of BVOC emissions, it still brings uncertainty to the simulation in this study. Future work can update the anthropogenic emission inventory and use dynamic meteorological data to explore multivariate effects and provide more accurate data for evaluating the roles of biogenic emissions in air quality. At the same time, the impact of meteorological changes on the long-term changes of BVOC emissions and formation of secondary air pollutants should also be considered to provide a scientific basis for the precise prevention and control of air pollution in response to climate change." is added.

References:

Climate Change Center of China Meteorological Administration: China Blue Book of Climate Change (2021), Science Press, Beijing, China, 2021.

Li, L., Yang, W., Xie, S., and Wu, Y.: Estimations and uncertainty of biogenic volatile organic compound emission inventory in China for 2008–2018, Sci. Total. Environ., 733, 139301, https://doi.org/10.1016/j.scitotenv.2020.139301, 2020.

Wang, H., Wu, Q. Z., Guenther, A. B., Yang, X. C., Wang, L. N., Xiao, T., Li, J., Feng, J. M., Xu, Q., and Cheng, H.: A long-term estimation of biogenic volatile organic compound (BVOC) emission in China from 2001–2016: the roles of land cover change and climate variability, Atmos. Chem. Phys., 21, 4825–4848, https://doi.org/10.5194/acp-21-4825-2021, 2021.

4. The logic is weak, and the text need to bere-organized. Each section in the results seems loose respectively, and the main line of the manuscript has not been highlighted. The topic is long term impacts variation, I think carry out the discussion in chronological order will be better. What's more, that disturbs the readers' thinking by posting the figure of spatial variations in BVOC emissions in Jun 2018 and explaining the emission situation in section 2.1.

Response: Thank you for your suggestion. In the revised manuscript, we revise the structure of Section 3 to make the contents clear. Section 3.1 "**BVOC emission**" is added by moving the relative content in Section 2.1 here to introduce the BVOC emissions in June 2018, discuss the change in leaf biomass and its influence on BVOC emissions from 1981 to 2018. Section 3.2 "**Impacts of BVOC emissions on O_3 and SOA**" mainly discusses the impact of BVOCs on MDA8 O_3 and SOA in June 2018, separately. In addition, contributions by BVOC component are discussed. Section 3.3 "**Interannual variability**" discusses the impact of interannual BVOC emission variations on O_3 and SOA formation caused by vegetation biomass variability in China during 1981–2018. **In this section, the contents are revised to be in chronological order in the revised manuscript.**

The relative description of BVOC emission characteristics is moved to the added Section 3.1 "**BVOC emission**" in line 164–204, as follows:

"**3.1 BVOC emission**

3.1.1 Spatial distributions of BVOC emissions

The total BVOC emissions in China estimated by MEGAN2.1 are 9.91 Tg in June 2018, of which isoprene, monoterpene, sesquiterpene, and other BVOCs account for 64.21%, 10.58%, 2.12%, and 23.09%, respectively. As shown in Fig. 1, BVOC emissions show significant spatial variations with the highest emissions in the Changbai Mountains, Greater Khingan Mountains, Qinling Mountains, the southeast and southwest China forest regions, and Hainan and Taiwan provinces, and the lowest in the Qinghai-Tibet Plateau and southern Xinjiang province.

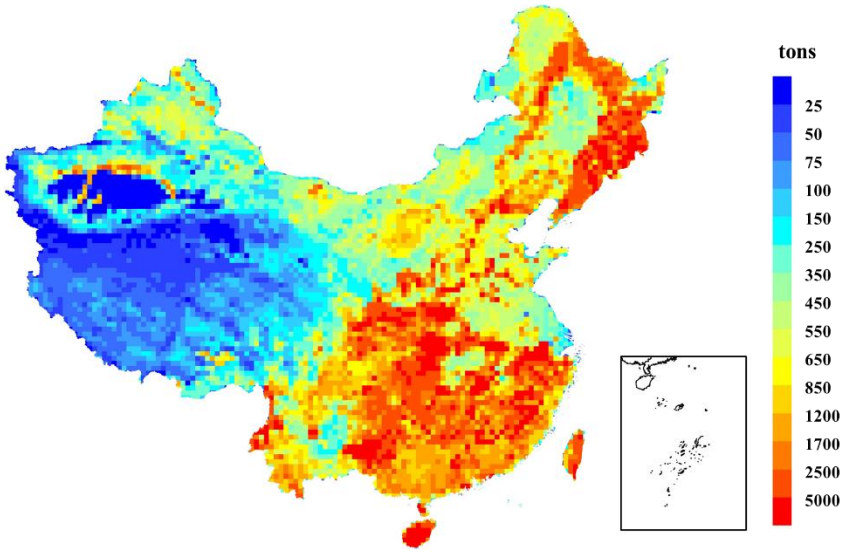

Fig. 1. Spatial variations in BVOC emissions in June 2018.

The emission simulations were validated by using the measurements of BVOC emission flux and formaldehyde (HCHO) concentration. The flux measurements of BVOCs conducted in China were collected (Bai et al., 2015, 2016, 2017). The gridded BVOC emission estimated by MEGAN were extracted where the flux measurement sites were located to do the comparison (Fig. S1). The modeled fluxes of BVOCs in this study capture the spatial variability of observations better with a correlation coefficient of 0.84. But the estimation is higher than measurement with an average mean bias of 1.11 mg m^{-2} h^{-1}, mainly because of the differences in time between them. Isoprene is the main compound in BVOC species, accounting for nearly half of total BVOC emissions in China. It undergoes chemical and photochemical reactions in the atmosphere, and the oxidation product is mainly HCHO (Bai and Hao, 2018; Orlando et al., 2000). In forest areas and in summer, biogenic isoprene is the dominant source of HCHO, so

satellite HCHO column concentration is widely used to constrain isoprene emissions (Opacka et al., 2021; Palmer et al., 2003; Stavrakou et al., 2018; Wang et al., 2021; Zhang et al., 2021). In this study, we used the HCHO vertical column detected by Ozone Monitoring Instrument (OMI) to validate the spatial variability of isoprene estimates. The monthly OMI HCHO data from the EU FP7 project QA4ECV product (Quality Assurance for Essential Climate Variables; http://www.qa4ecv.eu) was used in this study. The result of the statistical analysis with a confidence interval of 99% indicates that the monthly averaged OMI HCHO vertical column in June 2018 is significantly correlated to the model-estimated isoprene emissions.

3.1.2 Influence of leaf biomass variability

The leaf biomasses increased from 378.35 × 10^{12} g in 1981 to 1107.16 × 10^{12} g in 2018 at an average rate of 17.97 × 10^{12} g yr^{-1}. Among them, the forest and crop leaf biomass increased from 237.10 × 10^{12} to 518.38 × 10^{12} g and from 141.25 × 10^{12} to 588.79 × 10^{12} g, respectively, totally increasing by 192.63%. The spatial distribution of interannual variations in leaf biomass is presented in Fig. S2. The increase of leaf biomass is most significant in Great Khingan, Changbai Mountains, North China Plain, south and southwest China. This is mainly due to the increased stock of broadleaf and coniferous forests as a result of afforestation. Northern Qinghai-Tibet area and Northwest China have a relatively high grass cover rate but insignificant increase in leaf biomass of vegetation. It is because that the grass biomasses were the same over the historical simulations due to lacking of data.

Due to the increased volume and production of vegetation, the total BVOC emissions increased by 58.66% at average rates of 96.64 Gg yr^{-1}, of which isoprene, monoterpene, sesquiterpene increased by 108.57%, 38.17%, and 33.35% at average rates of 11.10, 0.99, and 0.17 Gg yr^{-1}, respectively. Isoprene emissions increased more rapidly over the past 40 years, which is primarily due to the greater increase in the biomass of broadleaf trees, which have the highest isoprene emission rates. Monoterpene and sesquiterpene increased at a lower rate because the increase of leaf biomass of conifers is relatively small. Fig. 2 shows the spatial distribution of interannual variations in BVOC emissions caused by the changing leaf biomass. Since the needleleaf and broadleaf trees tend to have a higher emission potential than grass or crop (Guenther et al., 2012), their wide distribution and the substantial increase in biomass result in the largest interannual variability of BVOC emissions in the Great Khingan, Changbai

Mountains, North China Plain, Central and Southern China, and Hainan Province. However, the emission of BVOCs in the northwest and southern coastal areas has decreased.

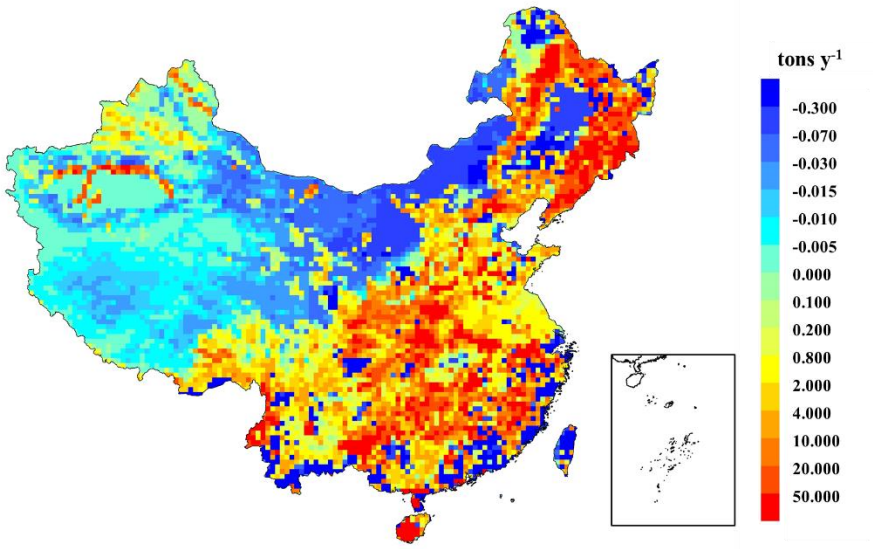

Fig. 2. Spatial distribution of interannual variations in BVOC emissions caused by leaf biomass changes."

Figures S1 and S2 are added to the Supplementary File.

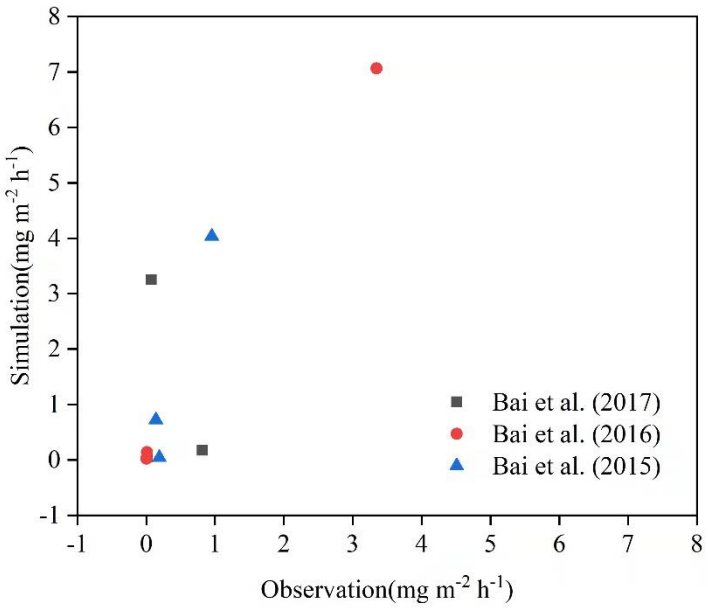

Fig. S1. Comparison of MEGAN model simulations with flux measurements in China.

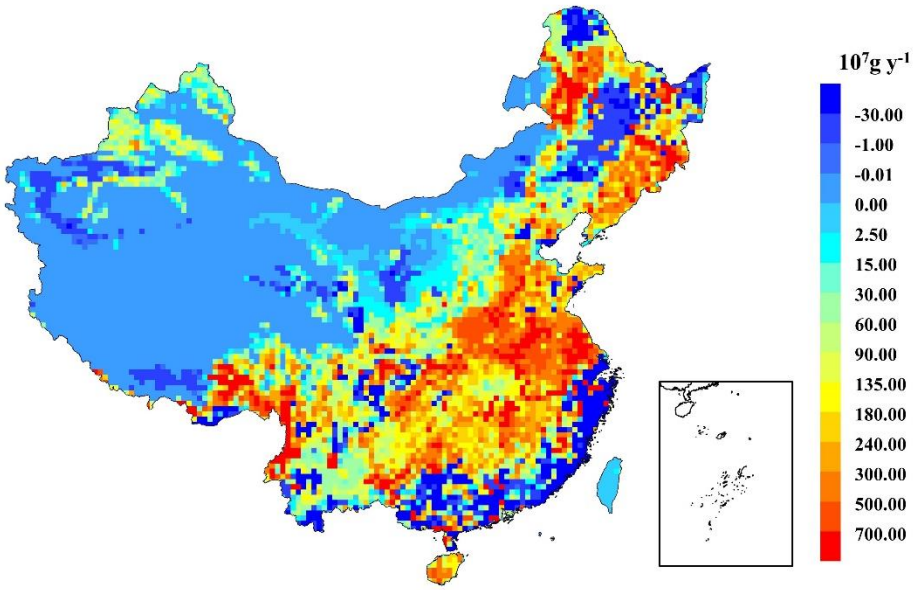

Fig. S2. Spatial distribution of interannual variations in leaf biomass.

In Section 3.2 and 3.3, some contents are revised to be in chronological order and make them logical.

Line 217–218, "Some areas in the west also have very small effect on O_3 formation by BVOC emissions." is deleted.

Line 331–332, "The growth was the most rapid in 2003 with an increase of 1.99% comparing with 1998." is revised to "Among the annual growth rates, the growth was the biggest in 2003 with an increase of 1.99% comparing with 1998.".

Line 339–347, "The lowest growth rate occurs in BTH. Due to the Three North Shelterbelt System Project, the area coverage of natural forest in the north of BTH has more than tripled than that in 2003, resulting in an increase in leaf biomass and BVOC emissions (Ma et al, 2019). However, because of the rapid urbanization in Beijing, a large amount of forest has been converted to urban construction land, and the reduction of BVOC emission related to losses of trees may offset part of their increase associated with rising coverage and volume in the surrounding areas. Although the largest O_3 enhancement occurs in PRD overall, MDA8 O_3 showed a significant decrease from 1981 to 1998 and an increase from 2013 to 2018. Under the influence of reform and opening in China, the vegetation leaf biomass in Guangdong Province has decreased from 25.48×10^{12} g to 6.92×10^{12} g by 72.81% during 1981–1998. The decrease of MDA8 O_3 in YRD is mainly due to the decrease of forest and cultivated biomass caused by

urbanization during 1994–2003." is revised to "At the end of the last century, the implementation of reform and opening up led to the continuous acceleration of the level of urbanization and the reduction of forest and arable land biomass and eventually resulting in the fluctuating decline of MDA8 O_3 in YRD and PRD during 1981–2003. The rapid growth of MDA8 O_3 in PRD led to a greater average annual growth rate of MDA8 O_3 in PRD greater than that in YRD from 1981 to 2018. The lowest growth rate occurs in BTH. Due to the Three North Shelterbelt System Project, the area coverage of natural forest in the north of BTH has more than tripled than that in 2003, resulting in an increase in leaf biomass and BVOC emissions (Ma et al, 2019). However, because of the rapid urbanization in Beijing, a large amount of forest has been converted to urban construction land, and the reduction of BVOC emission related to losses of trees may offset part of their increase associated with rising coverage and volume in the surrounding areas.".

Line 371–375, "With a similar overall growth rate, however, YRD and PRD have different interannual variability. In PRD, SOA showed a striking growth during the last five years owing to the increase of leaf biomass by up to 4.21×10^{12} g. YRD experienced two stages of increasing before and after 2003. In BTH, SOA annual growth rate is the lowest and lower than the national average rate. It can be attributed to the obvious decrease of leaf biomass with 17.57×10^{12} g from 1998 to 2008." is revised to "In BTH, SOA annual growth rate is the lowest and lower than the national average rate. It can be attributed to the obvious decrease of leaf biomass with 17.57×10^{12} g from 1998 to 2008. With a similar overall growth rate, however, YRD and PRD have different interannual variability. YRD experienced two stages of increasing before and after 2003. In PRD, SOA showed a striking growth during the last five years owing to the increase of leaf biomass by up to 4.21×10^{12} g.".

References:

Bai, J.H. and Hao, N.: The relationships between biogenic volatile organic compound (BVOC) emissions and atmospheric formaldehyde in a subtropical Pinus plantation in China, Ecology and Environmental Sciences, 27(6): 991–999, https://doi.org/10.16258/j.cnki.1674-5906.2018.06.001, 2018.

Bai, J., Guenther, A., Turnipseed, A., and Duhl, T.: Seasonal and interannual variations in

whole-ecosystem isoprene and monoterpene emissions from a temperate mixed forest in Northern China, Atmos. Pollut. Res., 6, 696–707, https://doi.org/10.5094/APR.2015.078, 2015.

Bai, J., Guenther, A., Turnipseed, A., Duhl, T., Y u, S., and Wang, B.: Seasonal variations in whole-ecosystem BVOC emissions from a subtropical bamboo plantation in China, Atmos. Environ., 124, 12–21, https://doi.org/10.1016/j.atmosenv.2015.11.008, 2016.

Bai, J., Guenther, A., Turnipseed, A., Duhl, T., and Greenberg, J.: Seasonal and interannual variations in whole-ecosystem BVOC emissions from a subtropical plantation in China, Atmos. Environ., 161, 176–190, https://doi.org/ 10.1016/j.atmosenv.2017.05.002, 2017.

Guenther, A. B., Jiang, X., Heald, C. L., Sakulyanontvittaya, T., Duhl, T., Emmons, L. K., and Wang, X.: The model of emissions of gases and aerosols from nature version 2.1 (MEGAN2.1): an extended and updated framework for modeling biogenic emissions, Geosci. Model Dev., 5, 1471–1492, https://doi.org/10.5194/gmd-5-1471-2012, 2012.

Ma, M., Gao, Y., Wang, Y., Zhang, S., Leung, L. R., Liu, C., Wang, S., Zhao, B., Chang, X., Su, H., Zhang, T., Sheng, L., Yao, X., and Gao, H.: Substantial ozone enhancement over the North China Plain from increased biogenic emissions due to heat waves and land cover in summer 2017, Atmos. Chem. Phys., 19, 12195–12207, https://doi.org/10.5194/acp-19-12195-2019, 2019.

Opacka, B., Müller, J.-F., Stavrakou, T., Bauwens, M., Sindelarova, K., Markova, J., and Guenther, A. B.: Global and regional impacts of land cover changes on isoprene emissions derived from spaceborne data and the MEGAN model, Atmos. Chem. Phys., 21, 8413–8436, https://doi.org/10.5194/acp-21-8413-2021, 2021.

Orlando, J. J., Nozière, B., Tyndall, G. S., Orzechowska, G. E., Grazyna, E., Paulson, S. E., and Rudich Y.: Product studies of the OH- and ozone-initiated oxidation of some monoterpenes, J. Geophys. Res., 105, 11561–11572, https://doi.org/10.1029/2000JD900005, 2000.

Palmer, P . I., Jacob, D. J., Fiore, A. M., Martin, R. V ., Chance, K., and Kurosu, T. P .: Mapping isoprene emissions over North America using formaldehyde column observations from space, J. Geophys. Res.-Atmos., 108, 4180, https://doi.org/10.1029/2002JD002153, 2003.

Stavrakou, T., Müller, J.-F., Bauwens, M., De Smedt, I., Van Roozendael, M., and Guenther, A.: Impact of Short-Term Climate Variability on Volatile Organic Compounds Emissions Assessed Using OMI Satellite Formaldehyde Observations, Geophys. Res. Lett., 45, 8681–8689, 2018.

Wang, H., Wu, Q. Z., Guenther, A. B., Yang, X. C., Wang, L. N., Xiao, T., Li, J., Feng, J. M., Xu, Q., and Cheng, H.: A long-term estimation of biogenic volatile organic compound (BVOC) emission in China from 2001–2016: the roles of land cover change and climate variability, Atmos. Chem. Phys., 21, 4825–4848, https://doi.org/10.5194/acp-21-4825-2021, 2021.

Zhang, M., Zhao, C., Yang, Y., Du, Q., Shen, Y., Lin, S., Gu, D., Su, W., and Liu, C.: Modeling sensitivities of BVOCs to different versions of MEGAN emission schemes in WRF-Chem (v3.6) and its impacts over eastern China, Geosci. Model Dev., 14, 6155–6175, https://doi.org/10.5194/gmd-14-6155-2021, 2021.

5. Overall the explanations are lack of mature and the scientific thinking is not

Response: Thank you for your suggestion. We are sorry for the insufficient explanation and discussion in the manuscript. We add the necessary discussion and explanation deeply to the results in the revised manuscript.

Line 223–232, "The positive contribution of BVOCs to O_3 in the southern region also confirms the conclusion that the VOCs-limited regime is dominant in southern China (Lu et al., 2019; Lyu et al., 2016; Tan et al., 2018). Because the dense population leads to a large number of NO_x emitted by human activities, NO_x is saturated with the formation of O_3 which is more sensitive to VOC emissions. Therefore, the higher BVOC emissions usually cause greater contribution to O_3 in these areas. To decrease BVOC emissions by planting plants with low emission potential may contribute to O_3 pollution control. From the spatial distribution of the BVOC effect (Fig. 2), the surface O_3 is sensitive to BVOC emissions in most regions in China which can furtherly indicate they are usually VOCs-limited. Comparing with the spatial distribution of BVOC emissions (Fig. 1), the areas with high BVOC emissions usually have a

higher contribution to O_3." is revised to "From the spatial distribution of the BVOC effect (Fig. 3), the surface O_3 is sensitive to BVOC emissions in most regions in China which can furtherly indicate they are usually VOCs-limited. It confirms the conclusion made by Lu et al. (2019), Lyu et al. (2016), and Tan et al. (2018) that the VOCs-limited regime is dominant in southern China. Comparing with the spatial distribution of BVOC emissions (Fig. 1), the areas with high BVOC emissions usually have a higher contribution to O_3. Because the dense population leads to a large number of NO_x emitted by human activities, NO_x is saturated with the formation of O_3 which is more sensitive to VOC emissions. Therefore, the higher BVOC emissions usually cause greater contribution to O_3 in these areas. In the VOC-limited regime, the reduction of VOC emissions reduces the chemical production of organic radicals (RO_2), which in turn lead to decreased cycling with NO_x and consequently lower concentration of O_3 (Jin and Holloway, 2015; Milford et al., 1989). To decrease BVOC emissions by planting plants with low emission potential may contribute to O_3 pollution control.".

Line 238–241, "These four key areas are populous, economically developed, and power grids are dense. The high concentration of NO_x emissions may lead to saturation of NO_x and excessive consumption of OH, so ozone generation is more sensitive to VOC emissions (Jin and Holloway, 2015)." is added.

Line 301, "which mainly because of the low concentration of other precursors" is added.

Line 307, "due to the different ratios of the different BVOC components emissions" is added.

Line 363–365, "Due to the low monoterpene emission level with less distribution of needleleaf trees in Hainan, the growth of SOA is very small." is revised to "Because of the tropical climate in southwestern Yunnan and Hainan, needleleaf trees with greater monoterpene emission potential are less distributed and the change of leaf biomass is small, which led to small or even negative changes in the growth of SOA.".

References:

Jin, X., and Holloway, T.: Spatial and temporal variability of ozone sensitivity over China observed from the ozone monitoring instrument, J. Geophys. Res. -Atmos., 120, 7229–7246, https://doi.org/10.1002/2015jd023250, 2015.

Lu, H., Lyu, X., Cheng, H., Ling, Z., and Guo, H.: Overview on the spatial-temporal characteristics of the ozone formation regime in China, Environm. Sci.: Processes and Impacts, 21, 916–929, https://doi.org/10.1039/C9EM00098D, 2019.

Lyu, X. P., Chen, N., Guo, H., Zhang, W. H., Wang, N., Wang, Y., and Liu, M.: Ambient volatile organic compounds and their effect on ozone production in Wuhan, central China, Sci. Total Environ., 541, 200–209, https://doi.org/10.1016/j.scitotenv.2015.09.093, 2016.

Milford, J. B., Russell, A. G., and MCRAE, G. J.: A new approach to photochemical pollution-control: Implications of spatial patterns in pollutant responses to reductions in nitrogen-oxides and reactive organic gas emissions, Environ. Sci. Technol.,23(10), 1290–1301, https://doi.org/10.1021/es00068a017, 1989.

Tan, Z., Lu, K., Jiang, M., Su, R., Dong, H., Zeng, L., Xie, S., Tan, Q., and Zhang, Y.: Exploring ozone pollution in Chengdu, southwestern China: A case study from radical chemistry to O_3-VOC-NO_x sensitivity, Sci. Total Environ., 636, 775–786, https://doi.org/10.1016/j.scitotenv.2018.04.286, 2018.

6. Section 2.2: Using a table to list the model settings is better to list them in a paragraph

Response: Thank you for your valuable suggestion. We add a table as Table S1 in the revised manuscript to show the main parameterization options for physical and chemical schemes of the model setup.

Correspondingly, line 133–135, "The Purdue Lin microphysics scheme, the Rapid Radiative Transfer Model (RRTM) longwave radiation scheme, the Goddard shortwave radiation scheme, the Yonsei University (YSU) planetary boundary layer scheme, the Noah land surface scheme, and the Grell-Freitas cumulus parameterization scheme were used." is deleted. Line 133–134, "Main parameterization options for physical and chemical schemes of the model setup are listed in Table S1." is added.

Table S1. WRF-Chem configuration.

Parameter	Option
Microphysics	Purdue Lin et al. scheme
Long-wave radiation	RRTM scheme
Short-wave radiation	Goddard shortwave scheme
Surface layer	Monin-Obukhov theory
Land surface	Noah Land Surface Model
Cumulus parameter	Grell-Devenyi Ensemble scheme
Planetary Boundary Layer	YSU scheme
Gas phase chemistry scheme	NOAA/ESRL RACM
Aerosol chemistry scheme	VBS
Photolysis scheme	Fast-J

7. Table 2: Don't branch the percentages of BVOC contribution

Response: Thank you for your suggestion. The percentages are deleted in the revised Table 2, as follows.

Table 2. Emissions of each BVOC category and their corresponding contribution to MDA8 O_3 and SOA concentration in the five key regions of China in June 2018.

	BVOC category	China	BTH	FWP	PRD	YRD	CC
Emission (10^4 tons)	Isoprene	636.28	15.66	30.29	34.74	53.43	24.50
	Monoterpene	104.81	2.77	2.16	5.09	4.38	11.59
	Sesquiterpene	20.98	0.64	0.32	1.27	1.42	1.65
	Total BVOCs	990.91	29.23	40.67	46.29	74.18	51.32
Contribution to MDA8 O_3 (ppb)	Isoprene	7.01	3.42	18.01	16.81	12.55	20.49
	Monoterpene	1.17	1.74	0.32	4.07	2.92	6.89
	Sesquiterpene	0.16	0.93	-1.36	1.66	1.06	2.88
	Isoprenoid	7.77	2.94	17.43	16.34	14.23	24.55
	Total BVOCs	8.61	4.10	18.94	18.74	13.40	23.29
Contribution to SOA ($\mu g\ m^{-3}$)	Isoprene	0.25	0.20	0.53	0.95	0.63	0.91
	Monoterpene	0.52	0.45	0.72	1.21	0.62	1.59
	Sesquiterpene	0.22	0.21	0.26	0.49	0.31	0.75
	Isoprenoid	0.84	0.78	1.30	1.96	1.29	2.52
	Total BVOCs	0.84	0.74	1.29	1.96	1.27	2.51

8. The form of picture display should be strengthened

Response: Thank you for your suggestion. In the revised manuscript, Fig. 4–8 are revised to make them more clear. Firstly, in Fig. 4, 5, and 7, the five key regions are marked. Secondly, Fig. 6 and 8 are changed by adding a coordinate of the annual increasing rate to better display the differences in the five key regions.

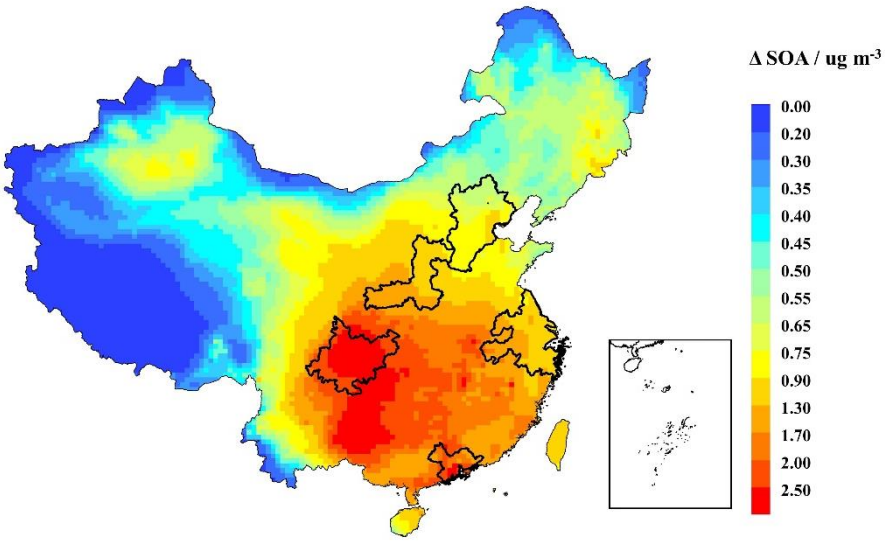

Fig. 4. Spatial variations in impact of BVOC emission on SOA concentration.

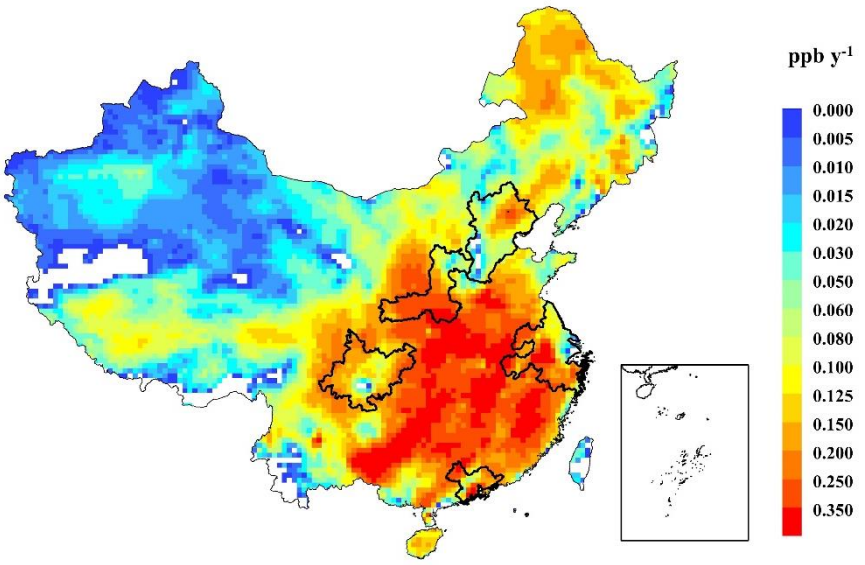

Fig. 5. Spatial distribution of interannual variations in O_3 simulated using annual BVOC emission factors.

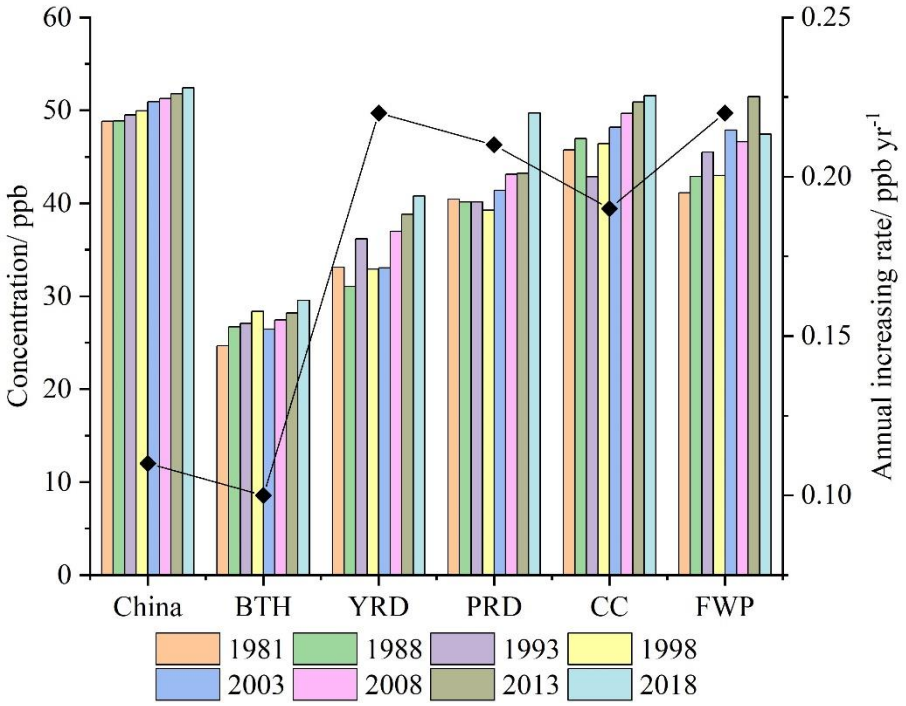

Fig. 6. The interannual changes of O_3 in China and the key regions.

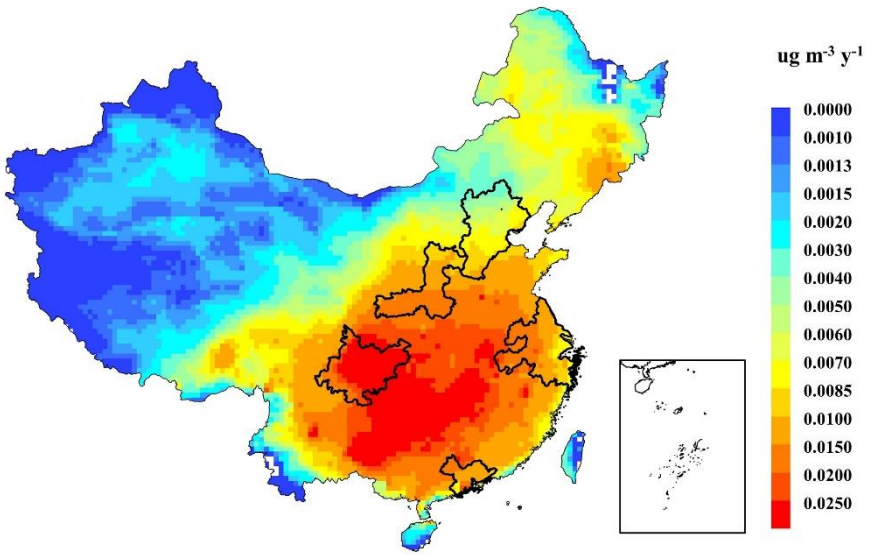

Fig. 7. Spatial distribution of interannual variations in SOA simulated using annual BVOC emission factors.

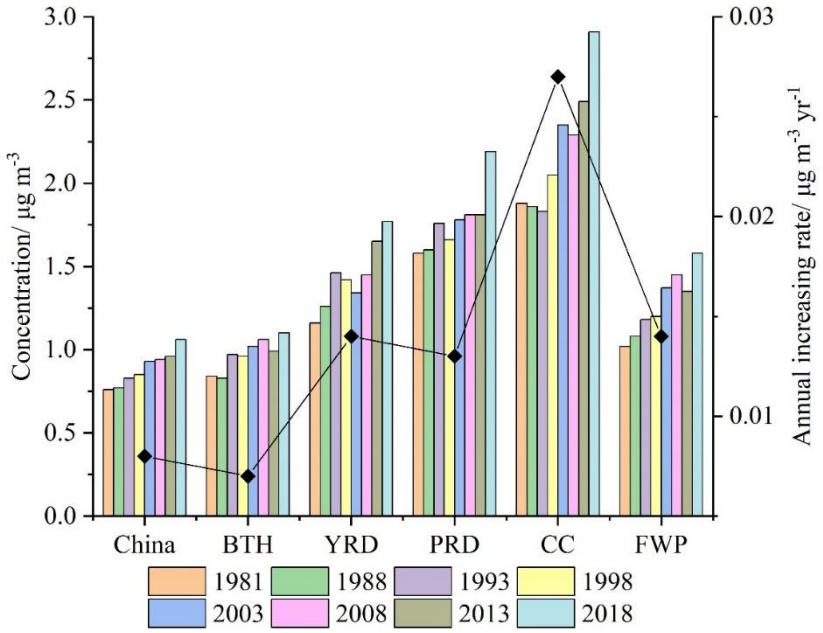

Fig. 8. The interannual changes of SOA in China and the key regions.

Response to Referee #2

1. Section 2.1: I recommend that you show a spatial map of changes in BVOCs over time? Li et al. (2020) shows only 2008-2018.

Response: Thank you for your valuable suggestion. In this study, the historical BVOC emissions were estimated using the same meteorology data to explore the influence of the interannual variability of vegetation biomass. So we add a spatial map of changes in BVOC emissions caused by vegetation biomass variability, as shown in Fig. 2. In addition, we add a new **Section 3.1 "BVOC emissions"** to describe the BVOC emissions in June 2018 and their interannual changes. The relative description of BVOC emissions in Section 2.1 of the original manuscript are moved here. In Section 3.1.2 "Sensitivity of the BVOC emissions to leaf biomass", Figure 2 is added and the changes in BVOC emissions caused by vegetation biomass variability are discussed.

Line 195–204 in revised manuscript, "Due to the increased volume and production of vegetation, the total BVOC emissions increased by 58.66% at average rates of 96.64 Gg yr^{-1}, of which isoprene, monoterpene, sesquiterpene increased by 108.57%, 38.17%, and 33.35% at average rates of 11.10, 0.99, and 0.17 Gg yr^{-1}, respectively. Isoprene emissions increased more rapidly over the past 40 years, which is primarily due to the greater increase in the biomass of broadleaf trees, which have the highest isoprene emission rates. Monoterpene and sesquiterpene increased at a lower rate because the increase of leaf biomass of conifers is relatively small. Fig. 2 shows the spatial distribution of interannual variations in BVOC emissions caused by the changing leaf biomass. Since the needleleaf and broadleaf trees tend to have a higher emission potential than grass or crop (Guenther et al., 2012), their wide distribution and the substantial increase in biomass result in the largest interannual variability of BVOC emissions in the Great Khingan, Changbai Mountains, North China Plain, Central and Southern China, and Hainan Province. However, the emission of BVOCs in the northwest and southern coastal areas has decreased."

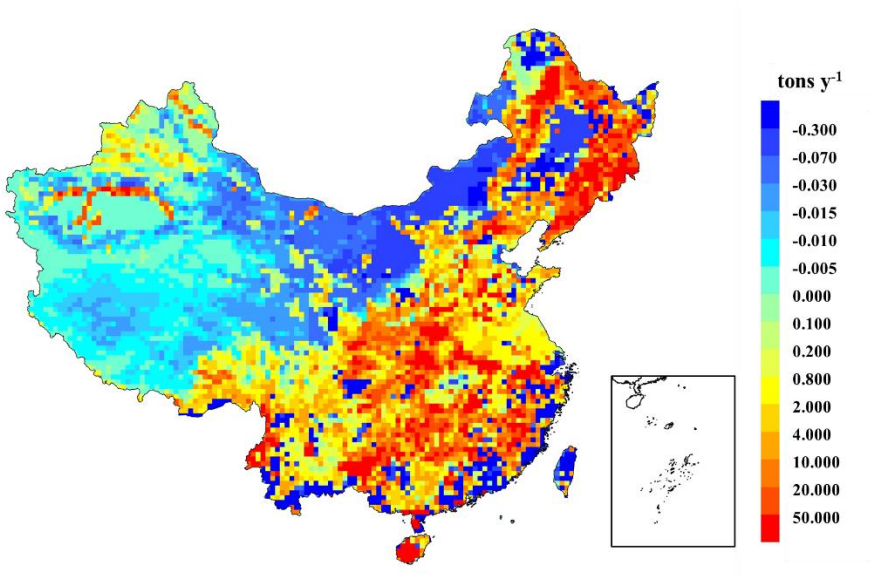

Fig. 2. Spatial distribution of interannual variations in BVOC emissions caused by leaf biomass changes.

References:

Guenther, A. B., Jiang, X., Heald, C. L., Sakulyanontvittaya, T., Duhl, T., Emmons, L. K., and Wang, X.: The model of emissions of gases and aerosols from nature version 2.1 (MEGAN2.1): an extended and updated framework for modeling biogenic emissions, Geosci. Model Dev., 5, 1471–1492, https://doi.org/10.5194/gmd-5-1471-2012, 2012.

2. In the introduction your say that your study uses "more accurate BVOC emissions". However, you don't provide evidence of this. Satellite data of formaldehyde could help in the evaluation over the satellite era. Do a literature search as there are a number of studies that use HCHO data to constrain BVOC emissions. How will you validate your emissions before the satellite era (e.g., 1981–2004)?

Response: Thank you for your constructive comment and we are sorry for the unclear explanation for our "more accurate BVOC emissions".

Firstly, we outstand the higher accuracy through comparing the method between our study and others in BVOC emission estimation. (1) **Determination of emission rate and leaf biomass.** In previous studies, traditional emission categories were used to determine isoprene

and monoterpene emission rates (Guenther et al., 1994; Klinger et al., 2002; Simpson et al., 1999; Wang et al., 2007). In this method, discrete emission categories (e.g., negligible, low, moderate, and high) were defined, which lacked theoretical evidence. And some studies utilized coarse emission intensity classifications. The determined emission rates typically differed between studies and had high uncertainty. In our study, we summarized a large number of observations from China and other countries to obtain more accurate basal emission rates by the theoretically effective statistical approach (Li et al., 2020). The statistical isoprene emission rates included seven categories by lowest, lower, low, moderate, high, higher, and highest. Monoterpene included six categories by lowest, lower, low, moderate, high, and higher. The accuracy of emission rates can be expected to be improved. For leaf biomass, the previous studies usually applied an average value for each vegetation class, such as broadleaf trees, needleleaf trees, crops, and grasses, without revealing their differences among regions and plant species (Klinger et al., 2002; Wang et al., 2007). In our study, the plant specific leaf biomasses were estimated based on the provincial or city-level statistic of vegetation volume and production using apportion models (Li and Xie, 2014). We obtained the gridded leaf biomass for the 23 vegetation species/types. (2) **Detailed vegetation classification.** Most studies on the BVOC emissions inventory in China typically include a coarse vegetation classification that is based on a less-detailed vegetation distribution (Gao et al., 2019; Klinger et al., 2002; Wang et al., 2007). And the MEGAN2.1 defined 15 vegetation types (Guenther et al., 2012). In our study, Vegetation Atlas of China (1:1,000,000), which had detailed vegetation distributions at a high horizontal resolution of about 250 m, was used to produce more detailed vegetation classification in Shandong Province, including 23 plant species/types (four broadleaf trees, five needleleaf trees, eight crop species, and six subtypes of shrub and grass).

In the revised manuscript, we add the explanation to show the higher accuracy of the determined emission factors and vegetation classification. Line 101–103, "Previous studies typically included a coarse vegetation classification that is based on a less-detailed vegetation distribution (Gao et al., 2019; Klinger et al., 2002; Wang et al., 2007). And the MEGAN2.1 defined 15 vegetation types by default (Guenther et al., 2012)." is added. Line 109–111, "In previous studies, traditional emission categories were used to determine emission rates (Guenther et al., 1994; Klinger et al., 2002; Simpson et al., 1999; Wang et al., 2007), which

usually utilized coarse categories and resulted in high uncertainty." is added. Line 113–115, "Previous studies usually applied an average value for each vegetation class, such as broadleaf trees, needleleaf trees, crops, and grasses, without revealing their differences among regions and plant species (Klinger et al., 2002; Wang et al., 2007)." is added.

Secondly, as you suggested, we add the validation of BVOC emissions by comparing the simulation with satellite observation of formaldehyde concentration and also the canopy-level emission flux measurements in China. The validation is conducted for estimation in 2018. The emissions in other years are not evaluated because the historical BVOC emissions are estimated using the same meteorology data to explore the influence of the interannual variability of vegetation biomass. They cannot display the real emissions for the years other than 2018. (1) Validation by comparing with canopy-level emission flux measurements. The canopy-level emission flux measurements in China were used for validation (Bai et al., 2015, 2016, 2017). The gridded BVOC emission estimated by MEGAN were extracted where locating the flux measurement sites. The comparison of model simulation and observation is shown in Fig. S1. The estimated of BVOC emissions are higher with an average mean bias of 1.11 mg m^{-2} h^{-1}, mainly because of the differences in time between the simulation and measurements. But they are correlated by r=0.84, exhibiting good agreement in spatial variations. (2) Validation by comparing with satellite observation of formaldehyde concentration. We compared simulated isoprene emission with satellite-derived HCHO column concentration using the Ozone Monitoring Instrument (OMI) HCHO vertical column product. The monthly averaged OMI HCHO vertical column in June 2018 correlates with the model estimated results at a 99% confidence level.

In the revised manuscript, the above validations are added in Section 3.1.1. Meanwhile, a literature summarization that use HCHO data to constrain BVOC emissions is also added. Line 171–185, "The emission simulations were validated by using the measurements of BVOC emission flux and formaldehyde (HCHO) concentration. The flux measurements of BVOCs conducted in China were collected (Bai et al., 2015, 2016, 2017). The gridded BVOC emission estimated by MEGAN were extracted where the flux measurement sites were located to do the comparison (Fig. S1). The modeled fluxes of BVOCs in this study capture the spatial variability of observations better with a correlation coefficient of 0.84. But the estimation is higher than

measurement with an average mean bias of 1.11 mg m^{-2} h^{-1}, mainly because of the differences in time between them. Isoprene is the main compound in BVOC species, accounting for nearly half of total BVOC emissions in China. It undergoes chemical and photochemical reactions in the atmosphere, and the oxidation product is mainly HCHO (Bai and Hao, 2018; Orlando et al., 2000). In forest areas and in summer, biogenic isoprene is the dominant source of HCHO, so satellite HCHO column concentration is widely used to constrain isoprene emissions (Opacka et al., 2021; Palmer et al., 2003; Stavrakou et al., 2018; Wang et al., 2021; Zhang et al., 2021). In this study, we used the HCHO vertical column detected by Ozone Monitoring Instrument (OMI) to validate the spatial variability of isoprene estimates. The monthly OMI HCHO data from the EU FP7 project QA4ECV product (Quality Assurance for Essential Climate Variables; http://www.qa4ecv.eu) was used in this study. The result of the statistical analysis with a confidence interval of 99% indicates that the monthly averaged OMI HCHO vertical column in June 2018 is significantly correlated to the model-estimated isoprene emissions." is added.

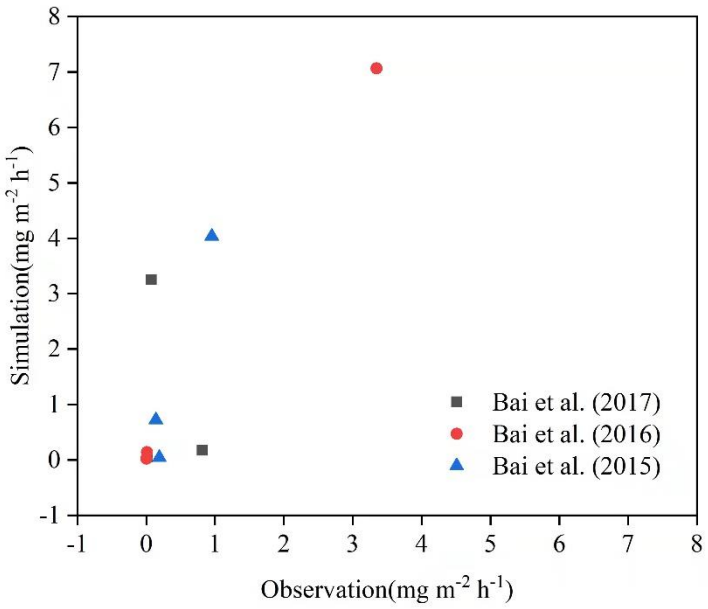

Fig. S1. Comparison of MEGAN model simulations with flux measurements in China.

References:

Bai, J., Guenther, A., Turnipseed, A., and Duhl, T.: Seasonal and interannual variations in whole-ecosystem isoprene and monoterpene emissions from a temperate mixed forest in

Northern China, Atmos. Pollut. Res., 6, 696–707, https://doi.org/10.5094/APR.2015.078, 2015.

Bai, J., Guenther, A., Turnipseed, A., Duhl, T., Y u, S., and Wang, B.: Seasonal variations in whole-ecosystem BVOC emissions from a subtropical bamboo plantation in China, Atmos. Environ., 124, 12–21, https://doi.org/10.1016/j.atmosenv.2015.11.008, 2016.

Bai, J., Guenther, A., Turnipseed, A., Duhl, T., and Greenberg, J.: Seasonal and interannual variations in whole-ecosystem BVOC emissions from a subtropical plantation in China, Atmos. Environ., 161, 176–190, 10.1016/j.atmosenv.2017.05.002, 2017.

Bai, J.H. and Hao, N.: The relationships between biogenic volatile organic compound (BVOC) emissions and atmospheric formaldehyde in a subtropical Pinus plantation in China, Ecology and Environmental Sciences, 27(6): 991-999, https://doi.org/10.16258/j.cnki.1674-5906.2018.06.001, 2018.

Gao, C., Zhang, X.L., Xiu, A.J., Huang, L., Zhao, H.M., Wang, K., and Tong, Q.Q.: Spatiotemporal distribution of biogenic volatile organic compounds emissions in China, Acta Sci. Circumst., 39, 4140–4151, https://doi.org/10.13671/j.hjkxxb.2019.0243, 2019.

Guenther, A. B., Jiang, X., Heald, C. L., Sakulyanontvittaya, T., Duhl, T., Emmons, L. K., and Wang, X.: The model of emissions of gases and aerosols from nature version 2.1 (MEGAN2.1): an extended and updated framework for modeling biogenic emissions, Geosci. Model Dev., 5, 1471–1492, https://doi.org/10.5194/gmd-5-1471-2012, 2012.

Guenther, A., Zimmerman, P., and Wildermuth, M.: Natural volatile organic compound emission rate estimates for U.S. woodland landscapes, Atmos. Environ., 28, 1197–1210, https://doi.org/10.1016/1352-2310(94)90297-6, 1994.

Klinger, L. F., Li, Q. J., Guenther, A. B., Greenberg, J. P ., Baker, B., and Bai, J. H.: Assessment of volatile organic compound emissions from ecosystems of China, J. Geophys. Res.-Atmos., 107, 16–21, https://doi.org/10.1029/2001jd001076, 2002.

Li, L. Y. and Xie, S. D.: Historical variations of biogenic volatile organic compound emission inventories in China, 1981–2003, Atmos. Environ., 95, 185–196, https://doi.org/10.1016/j.atmosenv.2014.06.033, 2014.

Li, L., Yang, W., Xie, S., and Wu, Y.: Estimations and uncertainty of biogenic volatile organic compound emission inventory in China for 2008–2018, Sci. Total. Environ., 733, 139301, https://doi.org/10.1016/j.scitotenv.2020.139301, 2020.

Opacka, B., Müller, J.-F., Stavrakou, T., Bauwens, M., Sindelarova, K., Markova, J., and Guenther, A. B.: Global and regional impacts of land cover changes on isoprene emissions derived from spaceborne data and the MEGAN model, Atmos. Chem. Phys., 21, 8413 – 8436, https://doi.org/10.5194/acp-21-8413-2021, 2021.

Orlando, J. J., Nozière, B., Tyndall, G. S., Orzechowska, G. E., Grazyna, E., Paulson, S. E., and Rudich Y.: Product studies of the OH- and ozone-initiated oxidation of some monoterpenes, J. Geophys. Res., 105, 11561–11572, https://doi.org/10.1029/2000JD900005, 2000.

Simpson, D. Winiwarter, W., Börjesson, G., Cinderby, S., Ferreiro, A., Guenther, A., Hewitt, C. N., Janson, R., Aslam K. Khalil, M., Owen, S., Pierce, T. E., Puxbaum, H., Shearer, M., Skiba, U., Steinbrecher, R., Tarrasón, L., and Öquist, M. G.: Inventorying emissions from Nature in Europe, J. Geophys. Res. A, 104, 8113–8152, https://doi.org/10.1029/98JD02747, 1999.

Stavrakou, T., Müller, J.-F., Bauwens, M., De Smedt, I., Van Roozendael, M., and Guenther, A.: Impact of Short-Term Climate Variability on Volatile Organic Compounds Emissions Assessed Using OMI Satellite Formaldehyde Observations, Geophys. Res. Lett., 45, 8681–8689, 2018.

Wang, H., Wu, Q. Z., Guenther, A. B., Yang, X. C., Wang, L. N., Xiao, T., Li, J., Feng, J. M., Xu, Q., and Cheng, H.: A long-term estimation of biogenic volatile organic compound (BVOC) emission in China from 2001–2016: the roles of land cover change and climate variability, Atmos. Chem. Phys., 21, 4825-4848, https://doi.org/10.5194/acp-21-4825-2021, 2021.

Wang, Q., Han, Z., Wang, T., and Higano, Y.: An estimate of biogenic emissions of volatile organic compounds during summertime in China, Environ. Sci. Pollut. Res., 14, 69–75, https://doi.org/10.1065/espr2007.02.376, 2007.

Zhang, M., Zhao, C., Yang, Y., Du, Q., Shen, Y., Lin, S., Gu, D., Su, W., and Liu, C.: Modeling sensitivities of BVOCs to different versions of MEGAN emission schemes in WRF-Chem (v3.6) and its impacts over eastern China, Geosci. Model Dev., 14, 6155–6175, https://doi.org/10.5194/gmd-14-6155-2021, 2021.

3. Table 1: Why do you use "Year 2008" for your "HISTORY" run, but "Year 2018" for the rest of your simulations?

Response: In the "HISTORY" simulation, we aimed to explore the impacts of interannual BVOC emission variations on O_3 and SOA formation caused by vegetation biomass variability during 1981–2018. In order to achieve this goal, we designed a scenario experiment by fixing meteorological data in one year and using the annual leaf biomass to drive BVOC estimates. The influences of annual meteorology on BVOC emissions and formation of secondary air pollutants were not considered. It is reported that vegetation change is the main driver of interannual variations of BVOC emissions (Li et al., 2020; Wang et al., 2021). The large-scale afforestation activities in recent years lead to the rapid increase of vegetation leaf biomass and therein BVOC emissions. In addition, the annual average temperature has a heating rate of 0.26 K per 10 years from 1951 to 2020 (Climate Change Center of China Meteorological Administration, 2021). Taking into account the long-term warming trend, we chose meteorological data of a mid-year 2008 over 1981–2018 as the constant input for historical simulation. The scenarios "BASE", "BIO", "ISOP", "MTP", "SQT", and "ISOPRENOID" were designed to simulate the impacts of emissions of BVOCs, isoprene, monoterpenes, sesquiterpenes, and isoprenoids (total of isoprene, monoterpene and sesquiterpene emissions) in June 2018 on O_3 and SOA, respectively. So we used the meteorology of 2018 to drive MEGAN to estimate the emissions in 2018.

We add the explanation in the revised manuscript. Line 156–157, "For these simulations, the meteorology of 2018 was used to drive MEGAN to estimate biogenic emissions in June 2018." is added. Line 159–162, "For the meteorology, the fixing set of a mid-year 2008 over 1981–2018 were used for all the HISTORY simulations. To explore the impacts of interannual BVOC emission variations caused by vegetation biomass variability, influences of annual

meteorology on BVOC emissions and formation of secondary air pollutants were not considered." is added.

References:

Climate Change Center of China Meteorological Administration: China Blue Book of Climate Change (2021), Science Press, Beijing, China, 2021.

Li, L., Yang, W., Xie, S., and Wu, Y.: Estimations and uncertainty of biogenic volatile organic compound emission inventory in China for 2008–2018, Sci. Total. Environ., 733, 139301, https://doi.org/10.1016/j.scitotenv.2020.139301, 2020.

Wang, H., Wu, Q. Z., Guenther, A. B., Yang, X. C., Wang, L. N., Xiao, T., Li, J., Feng, J. M., Xu, Q., and Cheng, H.: A long-term estimation of biogenic volatile organic compound (BVOC) emission in China from 2001–2016: the roles of land cover change and climate variability, Atmos. Chem. Phys., 21, 4825-4848, https://doi.org/10.5194/acp-21-4825-2021, 2021.

4. Line 176: Can you show a map of the simulated VOC to NOx ratio to help you make your point. Also, there are a number of papers discussing the VOC to NOx ratio over China, including as observed from space. For example: Jin, X., T. A. Holloway (2015). Spatial and temporal variability of ozone sensitivity over China observed from the Ozone Monitoring Instrument. Journal of Geophysical Research Atmospheres, 120(14), 7229–7246, doi: 10.1002/2015JD023250. Please do a literature search to see what they've concluded and if those conclusions are consistent with your study. It would also be helpful to show a spatial map of the simulated NOx distributions.

Response: Thank you very much for the constructive comment. In this study, we aim to explore the impact of interannual BVOC emission variations on O_3 and SOA caused by vegetation biomass variability. The impact of anthropogenic emissions was not considered. WRF-Chem model was run by fixing the anthropogenic emissions and meteorological data in a mid-year 2008 over 1981–2018. So we do not show the map of the simulated VOC to NO_x ratio and NO_x distribution, considering that there may be deviations with reality. However, we

do literature searches discussing the VOC to NO_x ratio over China to explain our results (Jin and Holloway, 2015; Lu et al., 2019; Lyu et al., 2016; Tan et al., 2018; Milford et al., 1989; Wang et al., 2008).

In the revised manuscript, we revise the relevant contents and made a more scientific explanation in line 218–235: "The spatial pattern of estimated MDA8 O_3 impacted by BVOC emissions differs from the spatial distribution of BVOC emissions mainly because of the variability of the nonlinear response relationship between O_3 formation and precursors. As the important precursors, VOCs and NO_x react in the presence of hydroxyl (OH) and hydroperoxyl (HO_2) radicals to create O_3. The O_3 formation is expected to be affected by the different levels of O_3 precursors in different land use functional areas. According to different VOCs/ NO_x ratio, O_3 formation regimes can be classified into VOC-limited (VOC-sensitive), transition, and NO_x-limited (NO_x-sensitive) regimes (Lu et al., 2019; Wang et al., 2008). From the spatial distribution of the BVOC effect (Fig. 3), the surface O_3 is sensitive to BVOC emissions in most regions in China which can furtherly indicate they are usually VOCs-limited. It confirms the conclusion made by Lu et al. (2019), Lyu et al. (2016), and Tan et al. (2018) that the VOCs-limited regime is dominant in southern China. Comparing with the spatial distribution of BVOC emissions (Fig. 1), the areas with high BVOC emissions usually have a higher contribution to O_3. Because the dense population leads to a large number of NO_x emitted by human activities, NO_x is saturated with the formation of O_3 which is more sensitive to VOC emissions. Therefore, the higher BVOC emissions usually cause greater contribution to O_3 in these areas. In the VOC-limited regime, the reduction of VOC emissions reduces the chemical production of organic radicals (RO_2), which in turn lead to decreased cycling with NO_x and consequently lower concentration of O_3 (Jin and Holloway, 2015; Milford et al., 1989). To decrease BVOC emissions by planting plants with low emission potential may contribute to O_3 pollution control. Notably, both northeastern and southern regions have the highest BVOC emissions, but their contributed O_3 differ much, which indicates that O_3 formation in the south is more sensitive to VOCs than in the northeast. Hainan province also has higher BVOC emissions but relatively lower contribution to O_3."

References:

Jin, X., and Holloway, T.: Spatial and temporal variability of ozone sensitivity over China observed from the ozone monitoring instrument, J. Geophys. Res. -Atmos., 120, 7229–7246, https://doi.org/10.1002/2015jd023250, 2015.

Lu, H., Lyu, X., Cheng, H., Ling, Z., and Guo, H.: Overview on the spatial-temporal characteristics of the ozone formation regime in China, Environm. Sci.: Processes and Impacts, 21, 916–929, https://doi.org/10.1039/C9EM00098D, 2019.

Lyu, X. P., Chen, N., Guo, H., Zhang, W. H., Wang, N., Wang, Y., and Liu, M.: Ambient volatile organic compounds and their effect on ozone production in Wuhan, central China, Sci. Total Environ., 541, 200–209, https://doi.org/10.1016/j.scitotenv.2015.09.093, 2016.

Milford, J. B., Russell, A. G., and MCRAE, G. J.: A new approach to photochemical pollution-control: Implications of spatial patterns in pollutant responses to reductions in nitrogen-oxides and reactive organic gas emissions, Environ. Sci. Technol.,23(10), 1290–1301, https://doi.org/10.1021/es00068a017, 1989.

Tan, Z., Lu, K., Jiang, M., Su, R., Dong, H., Zeng, L., Xie, S., Tan, Q., and Zhang, Y.: Exploring ozone pollution in Chengdu, southwestern China: A case study from radical chemistry to O_3-VOC-NO_x sensitivity, Sci. Total Environ., 636, 775–786, https://doi.org/10.1016/j.scitotenv.2018.04.286, 2018.

Wang, Q. G., Han, Z. W., Wang, T. J., and Zhang, R. J.: Impacts of biogenic emissions of VOC and NO_x on tropospheric ozone during summertime in eastern China, Sci. Total. Environ., 395, 41–49, https://doi.org/10.1016/j.scitotenv.2008.01.059, 2008.

5. Line 192: Can you mark (with boxes, for instance) the 5 regions on one of the maps, such as Figure 2?

Response: Thank you for your valuable suggestion. In the revised manuscript, the five key regions are marked in Figures 4, 5, and 7.

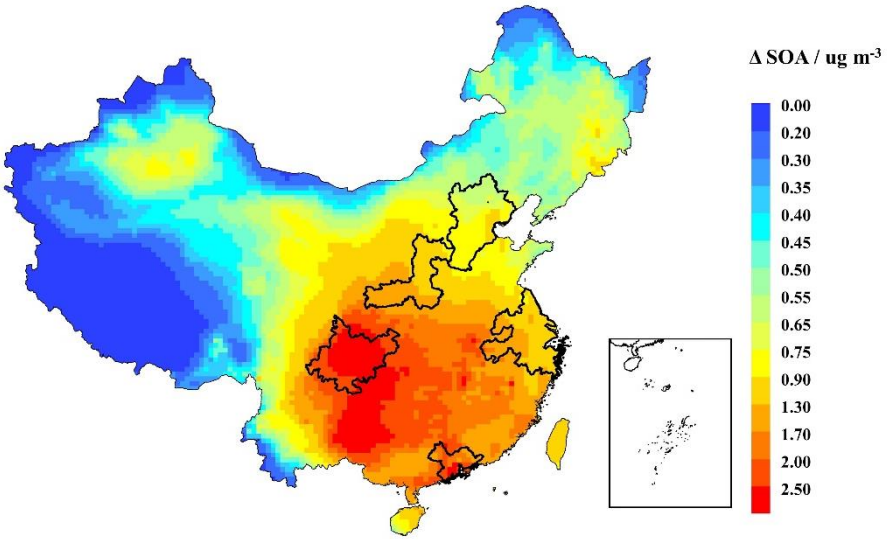

Fig. 4. Spatial variations in impact of BVOC emission on SOA concentration.

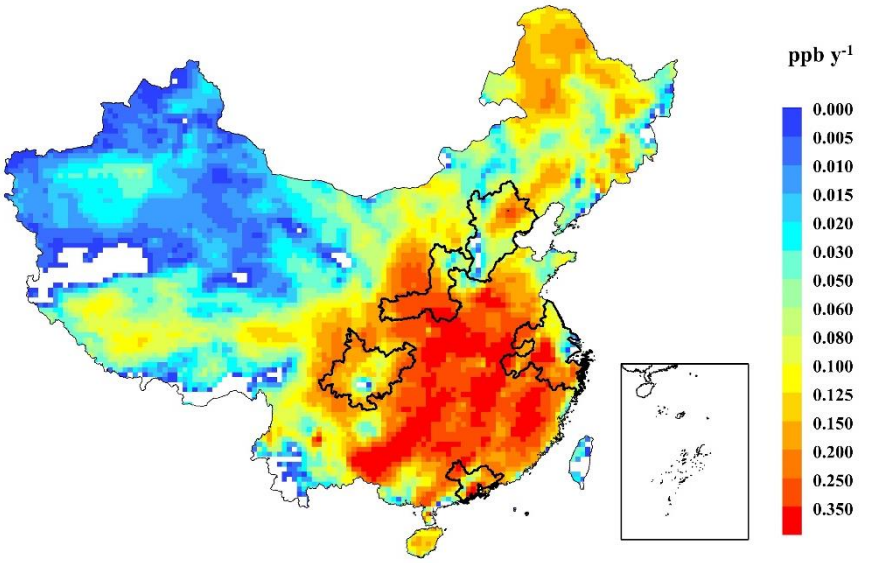

Fig. 5. Spatial distribution of interannual variations in O_3 simulated using annual BVOC emission factors.

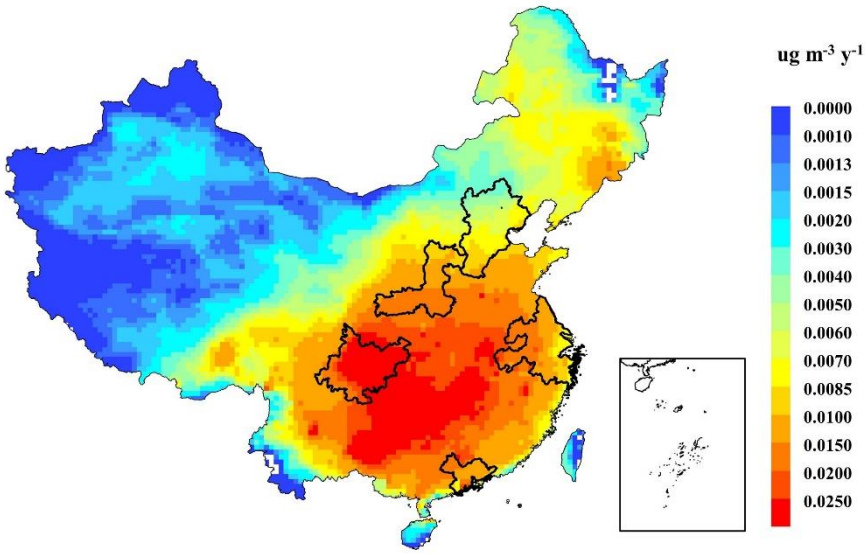

Fig. 7. Spatial distribution of interannual variations in SOA simulated using annual BVOC emission factors.

6. Line 245: "N3"? Do you mean NO3?

Response: We appreciate your careful reading very much and are sorry for the error. In revised manuscript, line 288, it is revised to "NO_3".

7. Line 275: You don't show the BVOCs emission changes for your study in "HISTORY". Why? A spatial map of the changes would be very helpful for the discussion.

Response: Thank you for your suggestion. In the revised manuscript, we add the detailed description of BVOC emission changes for the "HISTORY" simulation in **Section3.1.2**. The spatial map of the changes is also added as Fig. 2. In addition, the reason for the changes is discussed. The revisions can refer to the **Response to Comment 1 of Reviewer 2**.

8. Section 3.3.1: The discussion would be facilitated by maps (e.g., in supplementary material) of vegetation changes, leaf biomass changes, emission factors, etc.

Response: Thank you for your suggestion. In the revised manuscript, we add a spatial map of leaf biomass changes over 1981–2018 as Fig. S2. The vegetation distribution in our

estimations was derived from the Vegetation Atlas of China (1:1,000,000), which provides a detailed vegetation distribution at a high resolution. It was produced based on nationwide vegetation surveys and research from the past four decades and was published in 2007. It is rarely updated, and it represents the average distribution of vegetation in China. Therefore, the same PFT distribution was used to estimate BVOC emissions for 1981–2018 in this study. Emission factors were extrapolated by the leaf-level emission rates and leaf biomass using the canopy environment model described in MGEAN2.1. Emission rates were constant by time. So the interannual change of emission factor can be explained by that of leaf biomass.

Line 187–194 in revised manuscript, we add descriptions for the changes of leaf biomass: "The leaf biomasses increased from 378.35 × 10^{12} g in 1981 to 1107.16 × 10^{12} g in 2018 at an average rate of 17.97 × 10^{12} g yr^{-1}. Among them, the forest and crop leaf biomass increased from 237.10 × 10^{12} to 518.38 × 10^{12} g and from 141.25 × 10^{12} to 588.79 × 10^{12} g, respectively, totally increasing by 192.63%. The spatial distribution of interannual variations in leaf biomass is presented in Fig. S2. The increase of leaf biomass is most significant in Great Khingan, Changbai Mountains, North China Plain, south and southwest China. This is mainly due to the increased stock of broadleaf and coniferous forests as a result of afforestation. Northern Qinghai-Tibet area and Northwest China have a relatively high grass cover rate but insignificant increase in leaf biomass of vegetation. It is because that the grass biomasses were the same over the historical simulations due to lacking of data.".

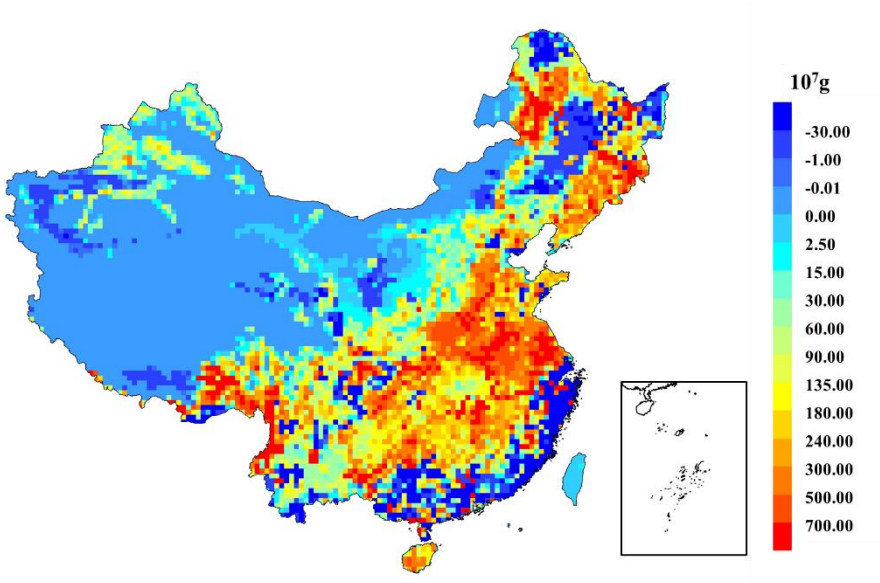

Fig. S2. Spatial distribution of interannual variations in leaf biomass.

Other modifications

1. Line 298–299, "For all the five regions, isoprene has both the largest emissions and the highest O_3 generation, followed by monoterpene and sesquiterpene." is revised to "For all the five regions, isoprene has both the largest emissions and the highest contribution of O_3 generation, followed by monoterpene and sesquiterpene.".

2. Line 360–361, "Hainan, and Taiwan provinces" is revised to " and Hainan provinces".

3. Line 361, "In these areas" is revised to "In northwestern areas".